Inorg. Chem. **2004**, *43*, 566–576

Molecular Paramagnetic Semiconductor: Crystal Structures and Magnetic and Conducting Properties of the Ni(dmit)$_2$ Salts of 6-Oxoverdazyl Radical Cations (dmit = 1,3-Dithiol-2-thione-4,5-dithiolate)

K. Mukai,*,† N. Senba,† T. Hatanaka,† H. Minakuchi,† K. Ohara,† M. Taniguchi,‡ Y. Misaki,‡ Y. Hosokoshi,§ K. Inoue,§ and N. Azuma†

Department of Chemistry, Faculty of Science, Ehime University, Matsuyama 790-8577, Graduate School of Engineering, Kyoto University, Kyoto 606-8501, and Institute for Molecular Science, Okazaki 444-8585, Japan

Received February 18, 2003

Four kinds of 1:1 and 1:3 salts of 3-[4-(trimethylammonio)phenyl]-1,5-diphenyl-6-oxoverdazyl radical cation ([**1**]$^+$) and its mono- and dimethyl derivatives ([**2**]$^+$ and [**3**]$^+$) with Ni(dmit)$_2$ anions (dmit = 1,3-dithiol-2-thione-4,5-dithiolate) ([**1**]$^+$[Ni(dmit)$_2$]$^-$ (**4**), [**2**]$^+$[Ni(dmit)$_2$]$^-$ (**5**), [**3**]$^+$[Ni(dmit)$_2$]$^-$ (**6**), and [**1**]$^+$[Ni(dmit)$_2$]$_3^-$ (**7**)) have been prepared, and the magnetic susceptibilities (χ_M) have been measured between 1.8 and 300 K. The χ_M values of salts **5** and **7** can be well reproduced by the sum of the contributions from (i) a Curie–Weiss system with a Curie constant of 0.376 (K emu)/mol and negative Weiss constants (Θ) of –0.4 and –1.7 K and (ii) a dimer system with strong negative exchange interactions of $2J/k_B = -354$ and –258 K, respectively. The dimer formations in Ni(dmit)$_2$ anions have been ascertained by the crystal structure analyses of salts **4**–**6**. In salts **4** and **6**, Ni(dmit)$_2$ dimer molecules are sandwiched between two verdazyl cations, indicating the formation of a linear tetramer in **4** and **6**. The magnetic susceptibility data for salts **4** and **6** have been fitted to a linear tetramer model using an end exchange interaction of $2J_1/k_B = -600$ K and a central interaction of $2J_2/k_B = -280$ K for **4** and $2J_1/k_B = -30$ K and $2J_2/k_B = -580$ K for **6**, respectively. The results of the temperature dependence of the $g(T)$ value in salts **4**–**6** obtained by ESR measurement also support the above analyses. The 1:1 salts **4**–**6** are insulators. On the other hand, the conductivity of the 1:3 salt **7** at 20 °C was $\sigma = 0.10$ S cm^{-1} with an activation energy $E_A = 0.099$ eV, showing the semiconductor property. Salt **7** is a new molecular paramagnetic semiconductor.

Introduction

Development of the molecular ferromagnet and that of the superconductor are two challenging targets in material science, and many studies have been performed with great success in recent years. Superconductivity and magnetism have long been considered incompatible with each other, because Cooper pairs are destroyed by an external field (or by the internal field generated in ferromagnets). Consequently, it is very interesting to establish superconductivity in a composite system containing localized magnetic moments. The first example of an organic/inorganic hybrid system in which paramagnetism and superconductivity coexist has been reported for (BEDT-TTF)$_4$(H$_2$O)[Fe(C$_2$O$_4$)$_3$](C$_6$H$_5$CN) [BEDT-TTF = bis(ethylenedithio)tetrathiafulvalene] ($T_C = 7$ K).[1] Coexistence of ferromagnetism and metallic conductivity has been found for a similar system, [BEDT-TTF]$_3$[MnCr(C$_2$O$_4$)$_3$].[2] Further, it has been reported that κ-BETS$_2$FeBr$_4$ (BETS = bis(ethylenedithio)tetraselenafulvalene) undergoes the transition from an antiferromagnetic (AFM) metal phase to a superconducting phase at 1.1 K.[3,4]

* Author to whom correspondence should be addressed. E-mail: mukai@chem.sci.ehime-u.ac.jp. Phone: 81-89-927-9588. Fax.: 81-89-927-9590.
† Ehime University.
‡ Kyoto University.
§ Institute for Molecular Science.

(1) Kurmoo, M.; Graham, A. W.; Day, P.; Coles, S. J.; Hursthouse, M. B.; Caulfield, J. L.; Singleton, J.; Pratt, F. L.; Hayes, W.; Ducasse, L.; Guionneau, P. *J. Am. Chem. Soc.* **1995**, *117*, 12209.
(2) Coronado, E.; Galan-Mascaros, J. R.; Gomez-Garcia, C. J.; Laukhin, V. *Nature* **2000**, *408*, 447.
(3) Fujiwara, H.; Fujiwara, E.; Nakazawa, Y.; Narymbetov, B. Z.; Kato, K.; Kobayashi, H.; Kobayashi, A.; Tokumoto, M.; Cassoux, P. *J. Am. Chem. Soc.* **2001**, *123*, 306.
(4) Ojima, E.; Fujiwara, H.; Kato, K.; Kobayashi, H.; Tanaka, H.; Kobayashi, A.; Tokumoto, M.; Cassoux, P. *J. Am. Chem. Soc.* **1999**, *121*, 5581.

10.1021/ic030068q CCC: $27.50
Published on Web 12/23/2003

However, the examples of the organic/inorganic hybrid system in which the magnetism and conductivity coexist are very limited, because of the difficulty in molecular design of the complexes.

Extensive studies have been performed for the assembled metal complexes (cation)$[M(dmit)_2]_2$ (M = Ni and Pd, and dmit = 1,3-dithiol-2-thione-4,5-dithiolate) of a closed-shell cation with an $M(dmit)_2$ anion, exhibiting insulating, metallic, and superconducting phases at low temperature under high pressure.[5−10] Two examples of molecular magnetic semiconductors consisting of an open-shell radical cation donor and a metal complex anion acceptor have been reported for the 1:1 salts of (i) the *p*-EPYNN (*p*-*N*-ethylpyridinium α-nitronyl nitroxide) and (ii) the Me_3N^+-TEMPO (*N*,*N*,*N*-trimethyl(1-oxyl-2,2,6,6-tetramethylpiperidine-4-yl)ammonium) radical cations with a $Ni(dmit)_2$ anion.[11,12]

Verdazyl radicals are well-known as one type of the representative stable free radicals. Several interesting magnetic properties, such as ferromagnetism,[13,14] weak ferromagnetism,[15−17] antiferromagnetism,[18] spin−Peierls transition,[19,20] and spin frustration,[21] have been found for the verdazyl radical crystals in recent years. The magnetic properties of the transition-metal and hydroquinone complexes of the verdazyl radicals have been investigated by Brook et al.[23,24] and Hicks et al.[25,26]

Chart 1

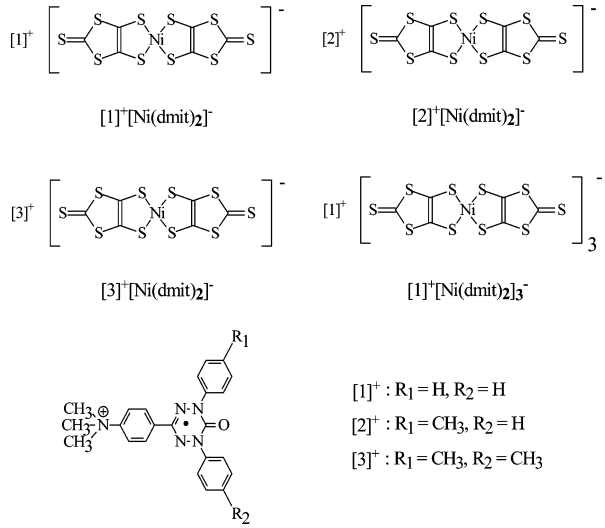

In a previous work, we reported the preparation of the 1:1 and 1:2 salts of ethylpyridinium verdazyl radical cations with TCNQ anion. The 1:2 salts were found to be genuine organic paramagnetic semiconductors.[27] Further, the 1:1 and 1:3 salts of $Ni(dmit)_2$ anion with 6-oxoverdazyl radical cation $[V]^+$ (V = 3-[4-(diethylmethylammonio)phenyl]-1,5-diphenyl-6-oxoverdazyl radical) were prepared.[28] The 1:1 and 1:3 salts were found to be a paramagnetic insulator and semiconductor, respectively. However, the examples of the molecular complexes consisting of the open-shell radical cation and $Ni(dmit)_2$ anion are very limited. In the present work, we prepared four kinds of $Ni(dmit)_2$ salts (**4**−**7**) of 3-[4-(trimethylammonio)phenyl]-1,5-diphenyl-6-oxoverdazyl radical cation ($[\mathbf{1}]^+$) and its mono- and dimethyl derivatives ($[\mathbf{2}]^+$ and $[\mathbf{3}]^+$) (see Chart 1), and studied the structural, magnetic, and electric properties of these radical salts.

Experimental Section

2. Experimental Section. Syntheses. 3-(4-Dimethylaminophenyl)-1,5-diphenyl-6-oxoverdazyl radical (*p*-DaDpOV) and its methyl derivatives (*p*-DaPTOV and *p*-DaDtOV) were prepared according to a procedure similar to that used by Neugebauer et al.[29] to prepare a 1,3,5-triphenyl-6-oxoverdazyl (TOV) radical. The precursors of the above verdazyl radicals, that is, 1,4,5,6-tetrahydro-2,4-diphenyl-6-(4-dimethylaminophenyl)-1,2,4,5-tetrazin-3(2*H*)-one and its methyl derivatives, were also prepared according to a method used by Neugebauer et al.[29]

3-(4-Dimethylaminophenyl)-1,5-diphenyl-6-oxoverdazyl, p-DaDpOV. To a stirred solution of 1,4,5,6-tetrahydro-6-(4-dimethylaminophenyl)-2,4-diphenyl-1,2,4,5-tetrazin-3(2*H*)-one (958 mg, 2.6 mmol) in dimethyl sulfoxide (5 mL) was added lead dioxide (4 g), and stirring was continued for 12 h. The reaction mixture was

(5) Brossard, L.; Ribault, M.; Valade, L.; Cassoux, P. *Physica B+C (Amsterdam)* **1986**, *143*, 378.
(6) Brossard, L.; Ribault, M.; Valade, L.; Cassoux, P. *J. Phys. (Paris)* **1989**, *50*, 1521.
(7) Kobayashi, A.; Kim, H.; Sasaki, Y.; Murata, K.; Kato, R.; Kobayashi, H. *J. Chem. Soc., Faraday Trans.* **1990**, *86*, 361.
(8) Cassoux, P.; Valade, L.; Kobayashi, H.; Kobayashi, A.; Clark, R. A.; Underhill, A. E. *Coord. Chem. Rev.* **1991**, *110*, 115.
(9) Pullen, A. E.; Olk, R.-M. *Coord. Chem. Rev.* **1999**, *188*, 211 and references are cited therein.
(10) Kato, R.; You-Liang, L.; Hosokoshi, Y.; Aonuma, S.; Sawa, H. *Mol. Cryst. Liq. Cryst.* **1997**, *296*, 217.
(11) Imai, H.; Otsuka, H.; Naito, T.; Awaga, K.; Inabe, T. *J. Am. Chem. Soc.* **1999**, *121*, 8098.
(12) Aonuma, S.; Casellas, H.; Faulmann, C.; Garreau de Bonneval, B.; Malfant, I.; Cassoux, P.; Lacroix, P. G.; Hosokoshi, Y.; Inoue, K. *J. Mater. Chem.* **2001**, *11*, 337.
(13) Mukai, K.; Konishi, K.; Nedachi, K.; Takeda, K. *J. Phys. Chem.* **1996**, *100*, 9658.
(14) Takeda, K.; Hamano, T.; Kawae, T.; Hidaka, M.; Takahashi, M.; Kawasaki, S.; Mukai, K. *J. Phys. Soc. Jpn.* **1995**, *64*, 2343.
(15) Kremer, R. K.; Kanellakopulos, B.; Bele, P.; Brunner, H.; Neugebauer, F. A. *Chem. Phys. Lett.* **1994**, *230*, 255.
(16) Tomiyoshi, S.; Yano, T.; Azuma, N.; Shoga, M.; Yamada, K.; Yamauchi, J. *Phys. Rev. B* **1994**, *49*, 16031.
(17) Mito, M.; Nakano, H.; Kawae, T.; Hitaka, M.; Takagi, S.; Deguchi, H.; Suzuki, K.; Mukai, K.; Takeda, K. *J. Phys. Soc. Jpn.* **1997**, *66*, 2147.
(18) Mito, M.; Takeda, K.; Mukai, K.; Azuma, N.; Gleiter, M. R.; Krieger, C.; Neugebauer, F. A. *J. Phys. Chem.* **1997**, *101*, 9517.
(19) Mukai, K.; Wada, N.; Jamali, J. B.; Achiwa, N.; Narumi, Y.; Kindo, K.; Kobayashi, T.; Amaya, K. *Chem. Phys. Lett.* **1996**, *257*, 538.
(20) Mukai, K.; Shimobe, Y.; Jamali, J. B.; Achiwa, N. *J. Phys. Chem. B* **1999**, *103*, 10876.
(21) Mukai, K.; Matsubara, M.; Hisatou, H.; Hosokoshi, Y.; Inoue, K.; Azuma, N. *J. Phys. Chem.* B **2002**, *106*, 8632.
(22) Mukai, K.; Nuwa, M.; Suzuki, K.; Nagaoka, S.; Achiwa, N.; Jamali, J. B. *J. Phys. Chem.* B **1998**, *102*, 782.
(23) Brook, D. J. R.; Lynch, V.; Conklin, B.; Fox, M. A. *J. Am. Chem. Soc.* **1997**, *119*, 5155.
(24) Brook, D. J. R.; Fornell, S.; Stevens, J. E.; Noll, B.; Kock, T. H.; Eisfeld, W. *Inorg. Chem.* **2000**, *39*, 562.
(25) Hicks, R. G.; Lemaire, M. T.; Thompson, L. K.; Barclay, T. M. *J. Am. Chem. Soc.* **2000**, *122*, 8077.
(26) Hicks, R. G.; Lemaire, M. T.; Ohrstrom, L.; Richardson, J. F.; Thompson, L. K.; Xu, Z. *J. Am. Chem. Soc.* **2001**, *123*, 7154.
(27) Mukai, K.; Jinno, S.; Shimobe, Y.; Azuma, N.; Hosokoshi, Y.; Inoue, K.; Taniguchi, M.; Misaki, Y.; Tanaka, K. *Polyhedron* **2001**, *20*, 1537.
(28) Mukai, K.; Hatanaka, T.; Senba, N.; Nakayashiki, T.; Misaki, Y.; Tanaka, K.; Ueda, K.; Sugimoto, T.; Azuma, N. *Inorg. Chem.* **2002**, *41*, 5066.
(29) Neugebauer, F. A.; Fischer, H.; Krieger, C. J. *J. Chem. Soc., Perkin Trans.* 2 **1993**, 535.

Table 1. Conductivity (σ_{RT}), Activation Energy (E_A), $\chi_M T$ Value (at 300 K), Magnetism, and Pascal's Diamagnetism (χ_{dia}) of Salts **4**−**10**

salt	σ_{RT} (S cm^{-1})	$\chi_M T$ [(K emu)/mol]	magnetism	$\chi_{dia}/10^{-3}$ (emu/mol)
[1]$^+$[Ni(dmit)$_2$]$^-$·$^1/_2$CH$_3$CN (**4**·$^1/_2$CH$_3$CN)	1.9×10^{-7} [a,c]	0.323 (0.391)[e]	linear tetramer ($T_{max} \approx 360$ K, $2J_1/k_B = -600$ K, $2J_2/k_B = -280$ K) + Curie impurity (3.0%)	−0.440
[2]$^+$[Ni(dmit)$_2$]$^-$ (**5**)	1.8×10^{-7} [a,c]	0.650	Curie−Weiss ($\Theta = -0.4$ K) + S−T ($2J/k_B = -354$ K)	−0.428
[3]$^+$[Ni(dmit)$_2$]$^-$ (**6**)	4.7×10^{-5} [b,d]	0.540	linear tetramer ($2J_1/k_B = -30$ K, $2J_2/k_B = -580$ K)	−0.440
[1]$^+$[Ni(dmit)$_2$]$_3^-$ (**7**)	1.0×10^{-1} [b,d] ($E_A = 0.10$ eV)	0.642	Curie−Weiss ($\Theta = -1.7$ K) + S−T ($2J/k_B = -258$ K)	−0.786
[1]$^+$I$^-$·$^1/_2$H$_2$O (**8**·$^1/_2$H$_2$O)		0.331	Curie−Weiss ($\Theta = -2.9$ K)	−0.287
[2]$^+$I$^-$ (**9**)		0.357	Curie−Weiss ($\Theta = -3.8$ K)	−0.297
[3]$^+$I$^-$ (**10**)		0.346	Curie−Weiss ($\Theta = -0.6$ K)	−0.312

[a] Single crystal. [b] Pressed pellet. [c] Two-probe ac method. [d] Four-probe ac method. [e] The value at 350 K.

filtered. After addition of water and chloroform to the filtrate the organic layer was separated, washed with water, dried ($MgSO_4$), and evaporated under reduced pressure. The residue was chromatographed on silica gel using chloroform as eluent. Recrystallization of the residue from ethyl acetate/*n*-hexane (1:3, v/v) afforded the product as dark-green thin needle crystals (787 mg, 83%): mp 184−186 °C; UV (dioxane) λ_{max} (log ϵ) 628 (3.01), 315 (4.60) nm. Anal. Found: C, 71.46; H, 5.48; N, 18.96. Calcd for $C_{22}H_{20}N_5O$: C, 71.33; H, 5.44; N, 18.91.

The following radicals were prepared similarly.

3-(4-Dimethylaminophenyl)-1-phenyl-5-tolyl-6-oxoverdazyl, *p-DaPTOV*. Light green thin needle crystals were obtained: mp 155−157 °C; UV (dioxane) λ_{max} (log ϵ) 625 (3.10), 315 (4.59) nm. Anal. Found: C, 71.94; H, 5.82; N, 18.13. Calcd for $C_{23}H_{22}N_5O$: C, 71.85; H, 5.77; N, 18.22.

3-(4-Dimethylaminophenyl)-1,5-ditolyl-6-oxoverdazyl, *p-DaDtOV*. Dark green needle crystals were obtained: mp 163−164 °C; UV (dioxane) λ_{max} (log ϵ) 625 (3.07), 316 (4.57) nm. Anal. Found: C, 72.50; H, 6.19; N, 17.55. Calcd for $C_{24}H_{24}N_5O$: C, 72.34; H, 6.07; N, 17.57.

Preparations of the iodide salts **8**−**10** were as follows.

[1]$^+$I$^-$ Salt (8), [1]$^+$ = 3-[4-(Trimethylammonio)phenyl]-1,5-diphenyl-6-oxoverdazyl Radical Cation. A 1.03 g sample of *p*-DaDpOV radical was dissolved in 20 mL of CH_3I, and the solution was stirred for 1 week at room temperature. The red crystals precipitated were filtered and washed with diethyl ether. Recrystallization of the residue from acetonitrile−diethyl ether solution afforded the product as dark-red plate crystals (1.35 g, 95%). The salt **8** includes a H_2O molecule in the crystal with a ratio of 1:0.5, as the crystal structure analysis indicates: mp 174−176 °C; UV (CH_3CN) λ_{max} (log ϵ) 535 (3.30), 424 (3.18), 314 (4.07), 248 (4.49) nm. Anal. Found: C, 53.37; H, 4.52; N, 13.42. Calcd for $C_{23}H_{23}N_5OI$·1/2H_2O: C, 52.98; H, 4.64; N, 13.43.

The following iodide salts were prepared similarly.

[2]$^+$I$^-$ Salt (9), [2]$^+$ = 3-[4-(Trimethylammonio)phenyl]-1-phenyl-5-tolyl-6-oxoverdazyl Radical Cation. Dark-red plate crystals were obtained: mp 150−152 °C; UV (CH_3CN) λ_{max} (log ϵ) 535 (3.35), 428 (3.23), 318 (4.07), 247 (4.50) nm. Anal. Found: C, 54.54; H, 4.83; N, 13.07. Calcd for $C_{24}H_{25}N_5OI$: C, 54.78; H, 4.78; N, 13.31.

[3]$^+$I$^-$ Salt (10), [3]$^+$ = 3-[4-(Trimethylammonio)phenyl]-1,5-ditolyl-6-oxoverdazyl Radical Cation. Dark-red plate crystals were obtained: mp 162−164 °C; UV (CH_3CN) λ_{max} (log ϵ) 535 (3.40), 433 (3.29), 322 (4.12), 247 (4.53) nm. Anal. Found: C, 55.31; H, 5.01; N, 13.00. Calcd for $C_{25}H_{27}N_5OI$: C, 55.56; H, 5.04; N, 12.96.

Preparations of the Ni(dmit)$_2$ salts **4**−**6** were as follows.

[1]$^+$[Ni(dmit)$_2$]$^-$ Salt (4). To a solution of [**1**]$^+$I$^-$ (16.1 mg, 0.0313 mmol) in acetonitrile (10 mL) was added slowly [*n*-Bu_4N]$^+$[Ni(dmit)$_2$]$^-$ (21.7 mg, 0.0313 mmol) in acetonitrile (20 mL), and the reaction mixture was kept for one night at room temperature under a nitrogen atmosphere. The dark green crystals of **4** (21.0 mg, 80%) precipitated were filtered and recrystallized from acetonitrile. The salt **4** includes a CH_3CN molecule in the crystal with a ratio of 1:0.5, as the crystal structure analysis indicates. Dark-green prismatic crystals were obtained: mp > 300 °C; UV (CH_3CN) λ_{max} (log ϵ) 618 (3.53), 572 (3.59), 540 (3.57), 438 (4.25), 392 (4.35), 314 (4.56), 238 (4.67) nm. Anal. Found: C, 42.09; H, 2.86; N, 8.98. Calcd for $C_{29}H_{23}N_5OS_{10}Ni$·$^1/_2CH_3CN$: C, 42.03; H, 2.88; N, 8.98.

The following Ni(dmit)$_2$ salts were prepared similarly.

[2]$^+$[Ni(dmit)$_2$]$^-$ Salt (5). Dark-green prismatic crystals were obtained: mp > 300 °C; UV (CH_3CN) λ_{max} (log ϵ) 615 (3.50), 574 (3.60), 547 (3.57), 440 (4.23), 392 (4.32), 316 (4.52), 237 (4.66) nm. Anal. Found: C, 42.23; H, 2.86; N, 8.31. Calcd for $C_{30}H_{25}N_5OS_{10}Ni$: C, 42.34; H, 2.96; N, 8.23.

[3]$^+$[Ni(dmit)$_2$]$^-$ Salt (6). Dark-green platelet crystals were obtained: mp > 300 °C; UV (CH_3CN) λ_{max} (log ϵ) 614 (3.48), 575 (3.58), 551 (3.56), 438 (4.20), 395 (4.28), 318 (4.49), 237 (4.63) nm. Anal. Found: C, 43.00; H, 3.12; N, 8.24. Calcd for $C_{31}H_{27}N_5OS_{10}Ni$: C, 43.04; H, 3.15; N, 8.10.

[1]$^+$[Ni(dmit)$_2$]$_3^-$ Salt (7). For the preparation of **7**, the air oxidation of a solution containing **4** (39 mg), acetic acid (15 mL), and acetic anhydride (15 mL) in acetone (150 mL) was carried out at room temperature.[8,9] Black fine crystals obtained show a high melting point and are insoluble in the usual organic solvents. The result of the elemental analysis indicates the formation of a 1:3 salt, **7**.[9] mp > 300 °C. Anal. Found: C, 28.24; H, 1.58; N, 3.66. Calcd for $C_{41}H_{23}N_5OS_{30}Ni_3$: C, 28.30; H, 1.33; N, 3.20.

Susceptibility and Conductivity Measurements. The magnetic susceptibility was measured in the temperature range of 1.8−300 K by a SQUID magnetometer. The susceptibility of all samples has been corrected for the diamagnetic contribution (χ_{dia}), calculated by Pascal's method (see Table 1).

The conductivity measurements were performed for the single crystals of salts **4** and **5** and the pressed pellet samples of salts **6** and **7**, using the standard two- or four-probe ac technique. Electrical contacts were achieved with gold paste.

Structure Determination and Crystal Data. The X-ray measurements of the Ni salts **4**−**6** and iodide salt **8** were carried out on a Rigaku AFC5R diffractometer with graphite-monochromated Cu Kα (λ = 1.54178 Å) and Mo Kα (λ = 0.71069 Å) radiations. The structure was solved by the direct method. The crystallographic data and the parameters of structure refinement are given in Table 2.

Results

UV and Visible Spectra of Salts 4−6. As reported in a previous work,[28] the absorption spectra of salts **4**−**6** in acetonitrile can be well explained by an addition of those of iodide salts **8**−**10** and [*n*-Bu_4N]$^+$[Ni(dmit)$_2$]$^-$, respectively, suggesting 1:1 complex formation between verdazyl cation

Table 2. Crystal Data, Experimental Conditions, and Refinement Details of the 1:1 $Ni(dmit)_2$ Salts **4**−**6** and the Iodide Salt **8**

	$[\mathbf{1}]^+[Ni(dmit)_2]^-\cdot{}^1/_2CH_3CN$	$[\mathbf{2}]^+[Ni(dmit)_2]^-$	$[\mathbf{3}]^+[Ni(dmit)_2]^-$	$[\mathbf{1}]^+I^-\cdot{}^1/_2H_2O$
empirical formula	$2(C_{23}H_{23}N_5O)2(C_6NiS_{10})\cdot C_2H_3N$	$C_{30}H_{25}N_5OS_{10}Ni$	$C_{31}H_{27}N_5OS_{10}Ni$	$C_{23}H_{23}N_5OI\cdot{}^1/_2H_2O$
fw	1714.74	850.94	864.97	521.38
cryst color	dark green, prismatic	dark green, prismatic	black, plate	red, prismatic
cryst syst	triclinic	triclinic	monoclinic	monoclinic
space group	$P\bar{1}$ (No. 2)	$P\bar{1}$ (No. 2)	$P2_1/c$ (No. 14)	$P2_1/n$ (No. 14)
a/Å	12.533(1)	13.281(3)	9.641(3)	13.114(4)
b/Å	15.012(2)	13.930(5)	22.435(4)	11.332(3)
c/Å	9.983(1)	10.618(4)	16.989(3)	18.437(7)
α/deg	97.632(10)	109.72(3)		
β/deg	107.299(8)	95.72(2)	93.37(2)	108.67(3)
γ/deg	89.890(10)	96.19(2)		
V/Å^3	1775.9(4)	1818.9(11)	3668(1)	2595.7(15)
Z	1	2	4	4
D_x/(g cm^{-3})	1.603	1.554	1.566	1.334
μ/cm^{-1}	65.76 (Cu Kα)	11.41 (Mo Kα)	11.33 (Mo Kα)	12.57 (Mo Kα)
cryst size/mm	0.280 × 0.180 × 0.150	0.300 × 0.200 × 0.150	0.50 × 0.38 × 0.08	0.430 × 0.230 × 0.130
range of 2θ/deg	4.7−123.1	4.7−55.1	4.7−55.0	4.7−55.0
no. of reflns measured	5813	8694	9147	6504
no. of unique reflns (R_{int})	5527 (0.015)	8377 (0.028)	8429 (0.058)	5970 (0.052)
no. of reflns obsd	5527 (all, $2\theta < 123.10°$)	8377 ($I > 0.00$)	6252 ($I > 2\sigma(F^2)$)	4908 ($I > 0.00$)
no. or reflns/no. of params ratio	12.94	19.76	14.44	17.53
R, R_w	0.041, 0.142	0.059, 0.156	0.087, 0.188	0.069, 0.212
S (goodness of fit)	0.98	1.18	1.22	1.15
max shifts/error	0.001	0.00	0.000	0.002
residual electron density/(e Å^{-3})	−0.52 to +0.40	−0.65 to +0.87	−1.18 to +1.57	−0.93 to +1.44

Table 3. Selected Structural Data for 1,3,5-triphenyl-6-oxoverdazyl (TOV), $[1]^+[Ni(dmit)_2]^-$ salt **4**, and **8**

	TOV	$[\mathbf{1}]^+[Ni(dmit)_2]^-\cdot{}^1/_2CH_3CN$[f]	$[\mathbf{1}]^+I^-\cdot{}^1/_2H_2O$
O−C2/Å	1.208(2)	1.212(4)	1.214(10)
N1−C2/Å[a]	1.381(1)	1.388(4)	1.39(1)
N1−N2/Å[b]	1.368(1)	1.366(4)	1.378(9)
N2−C1/Å[c]	1.330(1)	1.327(4)	1.34(1)
N5−C12/Å		1.500(4)	1.504(9)
N1−N2−C1/deg[d]	115.3	115.3(3)	113.7(7)
N2−C1−N3/deg	127.0	127.1(3)	128.9(7)
N3−N4−C2/deg[e]	124.0	124.4(3)	124.9(7)
N4−C2−N1/deg	114.4	113.5(3)	113.7(7)
dihedral angle/deg, N1-phenyl	34.5(1)	30.2(2)	41.3(3)
dihedral angle/deg, N4-phenyl	34.5(1)	53.8(1)	48.2(3)
dihedral angle/deg, C1-phenyl	12.3	9.5(1)	11.1(3)

[a] Mean value of N1−C2 and N4−C2. [b] Mean value of N1−N2 and N3−N4. [c] Mean value of N2−C1 and N3−C1. [d] Mean value of N1−N2−C1 and C1−N3−N4. [e] Mean value of N3−N4−C2 and C2−N1−N2. [f] C7, C8, and C18 atoms in salt **4** correspond to C1, C2, and C12 atoms in salt **8**, respectively.

and $[Ni(dmit)_2]^-$ anion. The **7** crystals are insoluble in the usual organic solvents, and we could not measure the optical spectrum of salt **7** in solution.

Crystal Structures of Salts 4−6 and 8. The crystal structure could be determined for the 1:1 $[V]^+[Ni(dmit)_2]^-$ (V = **1**−**3**) salts **4**−**6** and the salt **8** (see Table 2). Salts **4** and **8** include CH_3CN and H_2O molecules in the crystal with a ratio of 1:0.5, respectively. In parts a−c of Figure 1 and in Figure 2, we show the solid-state structures of salts **4**−**6** and **8**, respectively.

Table 3 shows that the bond lengths and bond angles of verdazyl moieties in the $Ni(dmit)_2$ salt **4** and iodide salt **8** are similar to those of the neutral 1,3,5-triphenyl-6-oxoverdazyl (TOV),[29] indicating that the verdazyl moieties in salts **4** and **8** are not oxidized.[30] The bond lengths and bond angles of verdazyl moieties in salts **5** and **6** are also similar to those of TOV (data are not shown). The structures of the $Ni(dmit)_2$ anion moiety in salts **4**−**6** are also similar to those in the $[n\text{-}Bu_4N]^+[Ni(dmit)_2]^-$ salt (data are not shown).[31] The dihedral angles between least-squares planes of two dmit rings in salts **4**−**6** are 4.38°, 8.11°, and 7.21°, respectively, indicating the planarity of the $Ni(dmit)_2$ moiety.

Molecular packing of salt **4** is shown in Figure 3. The unit cell of salt **4** contains two $Ni(dmit)_2$ anions and two verdazyl cations $[\mathbf{1}]^+$. The $Ni(dmit)_2$ anion molecules in salt **4** form a dimer ($[Ni(dmit)_2]$ (A)−$[Ni(dmit)_2]$ (B)) having intradimer contacts of ca. 3.6−3.7 Å along the b axis. The dimer molecules are sandwiched between two verdazyl cation $[\mathbf{1}]^+$ molecules, forming a linear tetramer ($[\mathbf{1}]^+$−$[Ni(dmit)_2]$ (A)−$[Ni(dmit)_2]$ (B)−$[\mathbf{1}]^+$) in the crystal (see Figure 3 and Table 4). The $Ni(dmit)_2$ anion dimers are connected to each other through short S−S contacts (S1−S1 = 3.632(2) Å and S1−S2 = 3.643(1) Å).

Molecular packing of salt **5** is shown in Figure 4. The unit cell of salt **5** contains two $Ni(dmit)_2$ anions and two verdazyl cations $[\mathbf{2}]^+$. The $Ni(dmit)_2$ anion molecules in salt **5** also form a dimer ($[Ni(dmit)_2]$ (A)−$[Ni(dmit)_2]$ (B)) having intradimer contacts of ca. 3.6−3.8 Å along the c axis (see Table 5). However, the interdimer distances are larger than 6.509(2) Å (S5−S10), as shown in Figure 4.

Molecular packing of salt **6** is shown in Figure 5. The unit cell of salt **6** contains four $Ni(dmit)_2$ anions and four verdazyl cations $[\mathbf{3}]^+$. The $Ni(dmit)_2$ anion molecules in salt **6** form a dimer ($[Ni(dmit)_2]$ (A)−$[Ni(dmit)_2]$ (B)) having intradimer contacts of ca. 3.6−3.8 Å presented in Table 6. The dimer molecules are sandwiched between two verdazyl cation $[\mathbf{3}]^+$ molecules, forming a linear tetramer ($[\mathbf{3}]^+$−$[Ni(dmit)_2]$ (A)−$[Ni(dmit)_2]$ (B)−$[\mathbf{3}]^+$) in the crystal, as observed for salt **4** (see Figure 5 and Table 6). The dimers are

(30) Nakatsuji, S.; Kitamura, A.; Takai, A.; Nishikawa, K.; Morimoto, Y.; Yasuoka, N.; Kawamura, H.; Anzai, H. *Z. Naturforsch.* **1998**, *53b*, 495.

(31) Lindqvist, O.; Anderson, L.; Sieler, J.; Steimecke, G.; Hoyer, E. *Acta Chem. Scand., Ser.* A **1982**, *36*, 855.

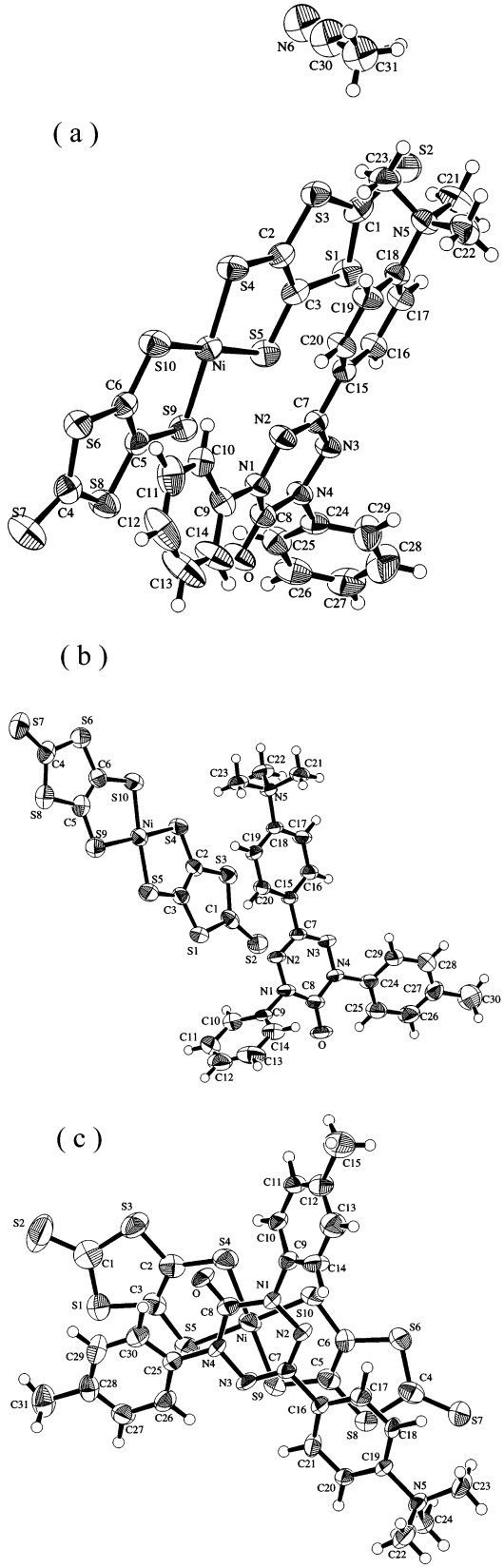

Figure 1. Molecular structure of (a) salt **4**, (b) salt **5**, and (c) salt **6** with the atom numbering scheme.

connected to each other through four short S−S contacts (S1−S8 = 3.803(4) Å, S5−S9 = 3.574(3) Å, S5−S8 = 3.747(4) Å, and S9−S9 = 3.586(5) Å), as shown in Figure 5.

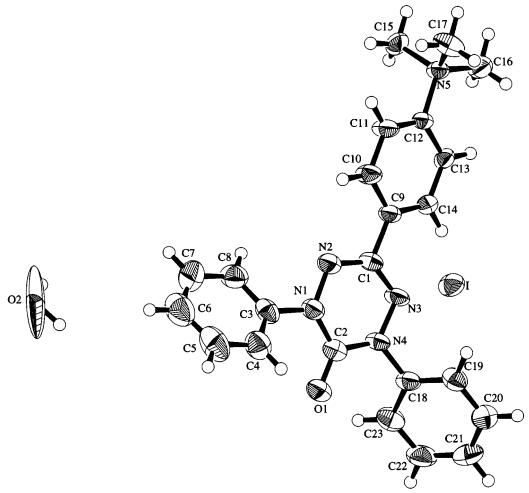

Figure 2. Molecular structure of the iodide salt **8** with the atom numbering scheme.

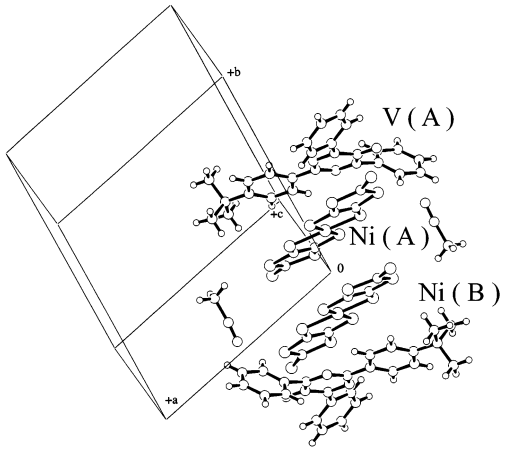

Figure 3. Molecular packing in salt **4**, showing the formation of a linear tetramer [verdazyl cation−Ni(dmit)$_2$ anion (A)−Ni(dmit)$_2$ anion (B)−verdazyl cation] along the *b* axis.

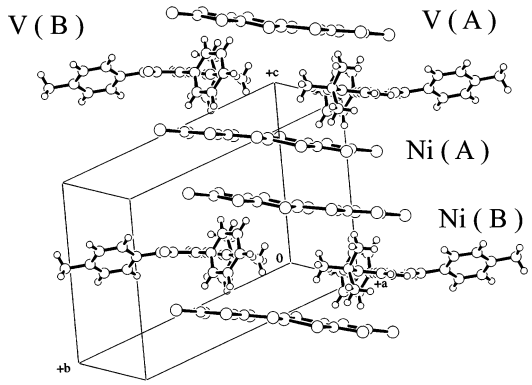

Figure 4. Molecular packing of salt **5**.

In the iodide salt **8**, the interatomic distances between the nitrogen atoms in the central hydrazidinyl moiety (N1−N2−C1−N3−N4−C2) having large unpaired spin densities are larger than 6.46(1) Å, indicating weak intermolecular exchange interaction, as described later.[32] The iodide ion (I^-) in salt **8** is located near the N3 and C1 atoms of the verdazyl ring; the I^-−N3 and I^-−C1 distances are 3.776(7) and

(32) Mukai, K.; Suzuki, K.; Ohara, K.; Jamali, J. B.; Achiwa, N. *J. Phys. Soc. Jpn.* **1999**, *68*, 3078.

Table 4. Pertinent Intermolecular Contacts (r/Å) in $[1]^+[Ni(dmit)_2]^-$ $\mathbf{4}\cdot{}^1/_2CH_3CN$

$[Ni(dmit)_2]\cdots[Ni(dmit)_2]$ [Ni(A)···Ni(B)]	$[Ni(dmit)_2]\cdots[Ni(dmit)_2]$ [Ni(A)···Ni(C)]	$[Ni(dmit)_2]\cdots$verdazyl [Ni(A)···V(A)]	$[Ni(dmit)_2]\cdots$verdazyl [Ni(A)···V(B)]	verdazyl···verdazyl
Ni···Ni, 5.540(1)	Ni···Ni, 9.98	Ni···N2, 3.853(3)	S7···N3, 3.690(3)	N*i*···N*j*, >5
Ni···S1, 3.679(1)	S1···S1, 3.632(2)	Ni···N3, 3.905(3)	S7···N4, 3.971(3)	
Ni···C3, 3.789(3)	S1···S2, 3.643(1)	S5···N3, 3.511(3)		
S2···C5, 3.877(4)	S1···C1, 3.834(4)	S9···N4, 3.429(3)		
S3···S9, 3.893(1)		S9···N1, 3.680(3)		
S4···S5, 3.945(1)		S9···N3, 3.791(3)		
S5···C2, 3.628(4)		S9···N2, 3.958(3)		
S5···C3, 3.772(4)		C5···N1, 3.584(4)		
S9···C1, 3.660(4)		C6···N1, 3.944(4)		

Table 5. Pertinent Intermolecular Contacts (r/Å) in **5**

$[Ni(dmit)_2]\cdots[Ni(dmit)_2]$ [Ni(A)···Ni(B)]	$[Ni(dmit)_2]\cdots$verdazyl [Ni(A)···V(A)]	$[Ni(dmit)_2]\cdots$verdazyl [Ni(A)···V(B)]	verdazyl···verdazyl
Ni···Ni, 4.390(2)	N*i*···N*j*, >5	S6···N2, 3.779(4)	N*i*···N*j*, >5
Ni···S4, 3.836(2)	S1···N2, 3.598(4)	S7···N4, 3.510(4)	
S1···S10, 3.916(2)	S2···N2, 3.716(4)	S7···N3, 3.570(4)	
S2···S6, 3.872(2)	S2···N4, 3.970(4)	S7···N1, 3.765(4)	
S2···S8, 3.918(2)		S7···N2, 3.825(4)	
S3···S9, 3.581(2)			
S4···S5, 3.767(2)			

Table 6. Pertinent Intermolecular Contacts (r/Å) in **6**

$[Ni(dmit)_2]\cdots[Ni(dmit)_2]$ [Ni(A)···Ni(B)]	$[Ni(dmit)_2]\cdots[Ni(dmit)_2]$ [Ni(A)···Ni(C)]	$[Ni(dmit)_2]\cdots$verdazyl [Ni(A)···V(A)]	$[Ni(dmit)_2]\cdots$verdazyl [Ni(A)···V(B)]	verdazyl···verdazyl
Ni···Ni, 4.603(3)	Ni···Ni, 6.516(3)	Ni···N4, 3.725(7)	S7···N2, 3.642(8)	N*i*···N*j*, >5
Ni···C2, 3.651(9)	S1···S8, 3.803(4)	Ni···N3, 3.821(8)	S7···N3, 3.682(8)	
Ni···S4, 3.754(3)	S5···S9, 3.574(3)	S4···N1, 3.971(7)	S7···N1, 3.745(7)	
S1···S10, 3.826(4)	S5···S8, 3.747(4)	S9···N3, 3.836(8)	S7···N4, 3.789(7)	
S2···S6, 3.987(6)	S9···S9, 3.586(5)	S10···N2, 3.657(8)		
S4···S5, 3.702(4)		S10···N1, 3.809(8)		
S10···C3, 3.773(9)		C6···N2, 3.87(1)		
S10···C1, 3.91(1)				
S10···C2, 3.944(9)				

3.765(8) Å, respectively. These values just correspond to the sum (3.73 and 3.83 Å) of the ionic radius (2.16 Å) of the I^- ion and the van der Waals radius (1.57 and 1.67 Å) of the N2 and C1 atoms, showing close contact between the I^- ion and N2 and C1 atoms, respectively. The increase of the g value in iodide salt **8** may be induced by the existence of the iodide ion. On the other hand, the distances ($I^-\cdots N5^+$ = 4.439(6), 4.591(6), and 5.069(6) Å) between the I^- ions and the neighboring nitrogen atoms ($N5^+$) having positive charge are larger than the above distances.

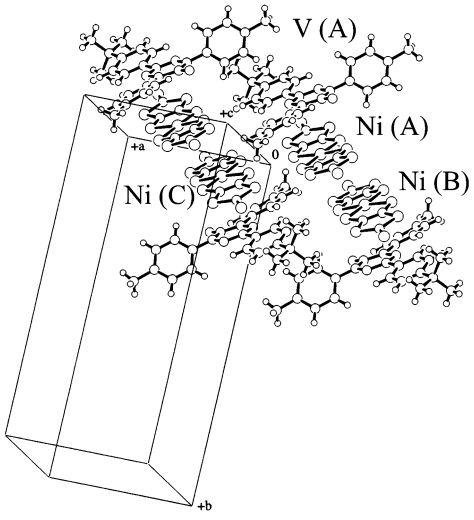

Figure 5. Molecular packing in salt **6**, showing the formation of a linear tetramer [verdazyl cation−Ni(dmit)$_2$ anion (A)−Ni(dmit)$_2$ anion (B)−verdazyl cation].

Conductivities of Salts 4−7. The room temperature conductivities (σ_{RT}) for salts **4**−**7** are 1.9×10^{-7}, 1.8×10^{-7}, 4.7×10^{-5}, and 1.0×10^{-1} S cm^{-1}, respectively, as listed in Table 1. Salts **4**−**6** are insulators as expected for the 1:1 salts. On the other hand, the 1:3 salt **7** has higher conductivity than the 1:1 salts. The temperature dependency of the resistivity of the 1:3 salt is shown in Figure 6. Under ambient pressure, the 1:3 salt **7** shows semiconductive behavior with

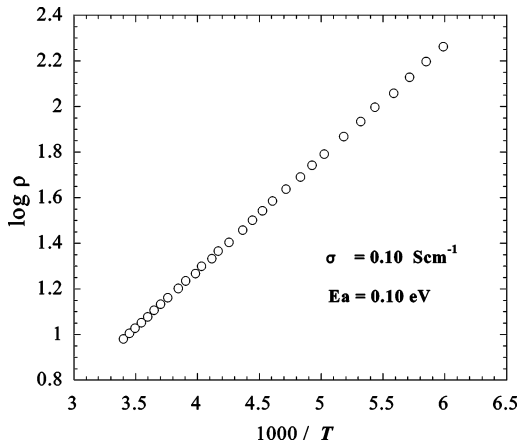

Figure 6. Temperature dependence of the resistivity (ρ) of the 1:3 salt **7** at ambient pressure.

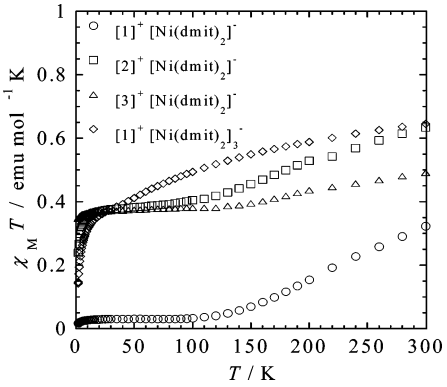

Figure 7. Temperature dependence of the product $\chi_M T$ for salts **4**−**7**.

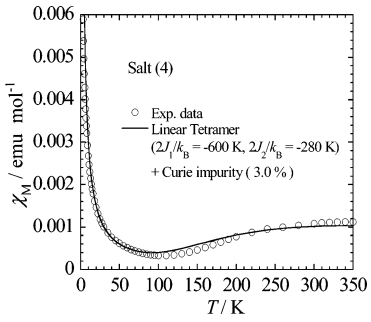

Figure 8. Temperature dependence of the magnetic susceptibility of salt **4**. The solid curve is the theoretical susceptibility calculated using eq 2 in ref 33.

an activation energy (E_A) of 0.10 eV in the temperature range of 165−300 K.

Magnetic Susceptibilities of Salts 4−10. Figure 7 shows a plot of $\chi_M T$ versus T for three kinds of 1:1 salts (**4**−**6**) and a kind of 1:3 salt (**7**). The values of $\chi_M T$ for **4**−**6** at 300 K are 0.323 (0.391 at 350 K), 0.650, and 0.540 K emu/mol, respectively. These values are larger than that (0.376 K emu/mol) for the $S = 1/2$ free spin system, suggesting that both spins of the verdazyl cation ($S = 1/2$) and $Ni(dmit)_2$ anion ($S = 1/2$) contribute to the magnetism of salts **4**−**6**. The χ_M of salt **4** shows a broad maximum at $T_{max} \approx 360$ K (see Figure 8). The susceptibilities of salts **5** and **6** increase monotonically with decreasing temperature from 300 K, and no peaks were observed in the susceptibilities. The susceptibility of the 1:3 salt **7** showed a behavior similar to that of the 1:1 salt **5**. The value (0.642 K emu/mol) of $\chi_M T$ at 300 K observed for salt **7** also suggests that both the spins of the verdazyl cation ($S = 1/2$) and $[Ni(dmit)_2]_3^-$ anion ($S = 1/2$) contribute to the magnetism of salt **7**.

The susceptibilities of the iodide salts **8**−**10** follow the Curie−Weiss law (see Table 1). The small value of the negative Weiss constant ($\theta = -2.9$ K) in salt **8** indicates weak AFM interaction. This agrees with the absence of short direct distances between the verdazyl moieties in salt **8**.

ESR Measurements of Salts 4−10. The ESR measurements were carried out in powder samples of salts **4**−**10** and $[n\text{-}Bu_4N]^+[Ni(dmit)]^-$ in the temperature range of 77−300 K. The g value and the peak-to-peak line width (ΔH_{PP}) of the samples at 300 and 77 K are listed in Table 7. The g values of the iodide salts **8**−**10** are nearly temperature independent (see Figure 9), while the line widths show a small increase with decreasing temperature. The g value and hyperfine splitting a^N of the iodide salts **8**−**10** in ethanol

Table 7. g value and Peak-to-Peak Line Width (ΔH_{PP}) of Salts **4**−**10** and Related Compounds

	300 K		77 K	
salt	g value	ΔH_{PP} (mT)	g value	ΔH_{PP} (mT)
4	2.0126[a]	24.9	2.0049[d]	13.8[d]
5	2.0159[a]	25.1	2.0044	0.869
6	2.0162[a]	21.4	2.0043	0.647
7				
8 (powder)	2.0048[b]	0.584	2.0048	0.603
8 (in EtOH)	2.0036[c]	$a^N = 0.57$ mT		
9 (powder)	2.0051[b]	0.854	2.0052	0.910
9 (in EtOH)	2.0036[c]	$a^N = 0.57$ mT		
10 (powder)	2.0061[b]	0.795	2.0060	0.918
10 (in EtOH)	2.0035[c]	$a^N = 0.57$ mT		
TOV (powder)	2.0039[b]			
TOV (in EtOH)	2.0036[c]	$a^N = 0.56$ mT		
$[n\text{-}Bu_4N]^+[Ni(dmit)_2]^-$	2.0472[a]	7.97	2.0474	7.94

[a] Experimental error ±0.0005. [b] Experimental error ±0.0002. [c] Experimental error ±0.0001. [d] The value at 123 K. At temperatures below 123 K, the anisotropic signal due to salt **4** appears, and the g value and line width could not be determined.

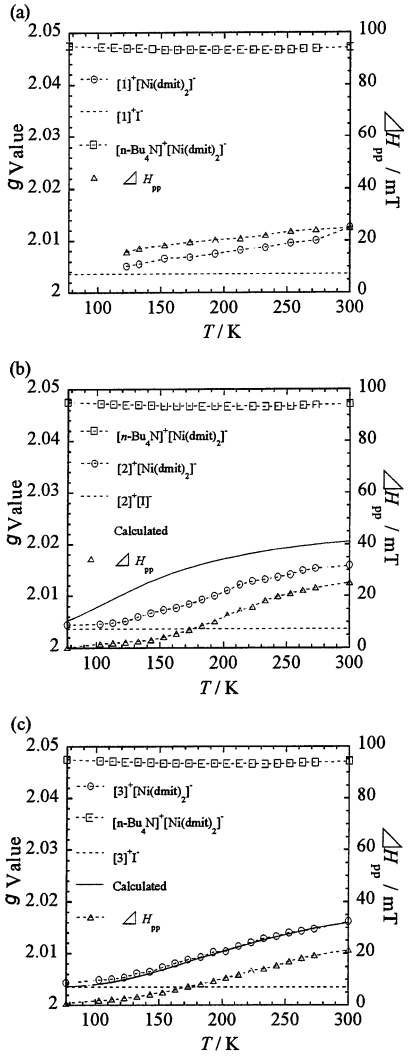

Figure 9. Temperature dependence of the g value ($g(T)$) (○) and the line width ($\Delta H_{PP}(T)$) (△) of the polycrystalline sample of (a) salt **4**, (b) salt **5**, and (c) salt **6**. The solid line is the theoretical $g(T)$ value calculated by using eq 4.

are similar to each other, and are similar to those ($g = 2.0036$ and $a^N = 0.56$ mT) of TOV radical. On the other hand, the g values ($g = 2.0048$, 2.0051, and 2.0061) of powder samples of salts **8**−**10** are larger than that (2.0039) of TOV. The I^- ion having a negative charge is located near the verdazyl ring in salt **8**, as described above. This negative charge may affect the increase of the g value of salt **8**. The $[n\text{-}Bu_4N]^+$-$[Ni(dmit)_2]^-$ salt exhibits one symmetric broad line ($g = 2.0472$ and $\Delta H_{PP} = 7.97$ mT) at 300 K. Both the g value and the line width are temperature independent (see Table 7 and Figure 9).

The ESR spectrum of salt **6** shows a symmetric broad line with a g value of 2.0162 and a line width of 21.4 mT at 300 K. However, in addition to the broad ESR signal of salt **6**, a symmetric single line ($g = 2.0045$ and $\Delta H_{PP} = 1.58$ mT) with a narrow line width which is attributable to the Curie impurity due to verdazyl radical cation was observed at 300 K. The integrated signal intensity of the Curie impurity was about 0.6% of that of salt **6**. The g value and the line width of salt **6** show notable temperature dependence, as shown in Figure 9c. Similarly, the salts **4** and **5** show a broad symmetric ESR absorption, and both the g value and the line width decrease with decreasing temperature, as shown in Figure 9a,b. On the other hand, the 1:3 salt **7** shows anisotropic absorption with an anomalous line shape at 77−300 K, and we could not determine the g value of salt **7**.

Discussion

Magnetic Property of Salt 4. The susceptibility of the salt shows a maximum at $T_{max} \approx 360$ K, and increases again below ca. 100 K with decreasing temperature, as shown in Figure 8. The increase in χ_M is probably due to the Curie impurity (3.0%) included in the crystal. The g value of salt **4** decreases from 2.0126 at 300 K to 2.0049 at 123 K by lowering the temperature, as shown in Figure 9a. The g value (2.0126) of **4** at 300 K is larger than that of verdazyl cation ($g_{V^+} = 2.0036$) and smaller than that of $Ni(dmit)_2$ anion ($g_{Ni^-} = 2.0472$) at 300 K, suggesting that both the spins of the cation and anion contribute to the magnetism of salt **4**. The g value (2.0049) of **4** at 123 K is similar to that (2.0036 in ethanol) of verdazyl radical cation. The result indicates that the verdazyl cation spins contribute mainly to the χ_M of salt **4** at 123 K.

The molecular packing of salt **4** is shown in Figure 3. As described in a previous section, the $Ni(dmit)_2$ anion molecules in salt **4** form a dimer ($Ni(dmit)_2$ (A)−$Ni(dmit)_2$ (B)) with short intradimer contacts of ca. 3.6−3.7 Å, suggesting strong AFM exchange interaction. However, the χ_M of **4** cannot be explained by a dimer model. In salt **4**, the dimer molecules are sandwiched between two verdazyl cation $[\mathbf{1}]^+$ molecules, forming linear tetramer ($[\mathbf{1}]^+$−$[Ni(dmit)_2]^-$ (A)−$[Ni(dmit)_2]^-$ (B)−$[\mathbf{1}]^+$) (see Figure 3 and Table 4). We can expect strong exchange interaction between the $Ni(dmit)_2$ anions and the verdazyl cations $[\mathbf{1}]^+$, because there are many short contacts between the Ni, S*i*, and C*i* atoms in the $Ni(dmit)_2$ anions and the N*j* atoms ($j = 1-4$) in the hydrazidinyl moiety (N1−N2−C7−N3−N4−C8), having large unpaired spin densities, of verdazyl cations $[\mathbf{1}]^+$.[32]

Chart 2

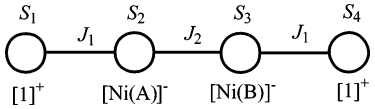

In such a case, the χ_M of salt **4** may be explained by a four-spin Heisenberg Hamiltonian

$$H = -2J_1(S_1S_2 + S_3S_4) - 2J_2S_2S_3 \quad (1)$$

$$S_1 = S_2 = S_3 = S_4 = 1/2$$

where J_1 is the exchange interaction between an edge verdazyl cation and a central $Ni(dmit)_2$ anion and J_2 is the interaction between two central $Ni(dmit)_2$ anions. The model is shown in Chart 2. This Hamiltonian has been solved exactly by Rubenacker et al.,[33] to obtain the energy levels and magnetic susceptibility. Using eq 2 in ref 33, we have fitted our data to this model, where, as the g value of salt **4**, the average value ($g_{av} = 2.0254$) of $g_{V^+} = 2.0036$ for the verdazyl cation and $g_{Ni^-} = 2.0472$ for the $Ni(dmit)_2$ anion was used tentatively for the calculation of the susceptibility. The calculated susceptibility is shown by the solid curve in Figure 8, where χ_{Curie} due to the Curie impurity (3.0%) included in the crystal was added to the theoretical susceptibility. The best fit parameters obtained are $2J_1/k_B = -600$ K and $2J_2/k_B = -280$ K. The $2J_2/k_B$ value (−280 K) for the dimer compares well with those (−354 and −580 K) for the $Ni(dmit)_2$ dimer in salts **5** and **6**, respectively, as described later.

Magnetic Properties of Salts 5 and 6. The susceptibilities of salts **5** and **6** can be reproduced by the sum of the two contributions, as shown in Figure 10a,b, respectively

$$\chi_M(T) = \chi_{Curie-Weiss}(T) + \chi_{S-T}(T) \quad (2)$$

where the first and second terms represent the contributions from (i) the Curie−Weiss system and (ii) the singlet−triplet (S−T) equilibrium system (dimer system), respectively. $\chi_{S-T}(T)$ is given by eq 3.

$$\chi_{S-T}(T) = (N_o g^2 \mu_B{}^2/k_B T)[1/(3 + e^{-2J/kBT})] \quad (3)$$

The solid curve in Figure 10a is a theoretical curve ((i) $C_{Curie} = 0.376$ (K emu)/mol and $\Theta = -0.4$ K and (ii) $2J_{A-B}/k_B = -354$ K) calculated for salt **5**. Similarly, the solid curve in Figure 10b is a theoretical curve ((i) $C_{Curie} = 0.376$ (K emu)/mol and $\Theta = -0.3$ K and (ii) $2J_{A-B}/k_B = -580$ K) calculated for salt **6**. The results show that the susceptibilities can be explained approximately by eq 2. The susceptibilities of salts **5** and **6** at the low-temperature region are due to the spins of verdazyl cations $[\mathbf{2}]^+$ and $[\mathbf{3}]^+$, respectively, because the $Ni(dmit)_2$ anions form a dimer in the crystal lattice, as described below.[9,11,12]

Figure 4 shows a projection of the structure of salt **5** along the a axis. The $Ni(dmit)_2$ anion molecules form a dimer, $Ni(dmit)_2$ (A)−$Ni(dmit)_2$ (B), having short interatomic

(33) Rubenacker, G. V.; Drumheller, J. E.; Emerson, K.; Willet, R. D. *J. Magn. Magn. Mater.* **1986**, *54*, 1483.

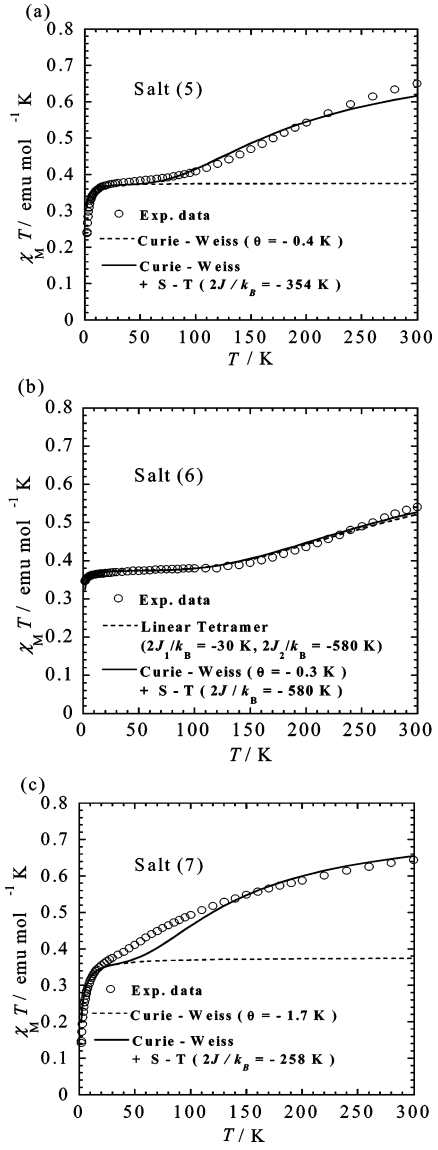

Figure 10. Temperature dependence of the product $\chi_M T$ (○) for (a) the 1:1 salt **5**, (b) the 1:1 salt **6**, and (c) the 1:3 salt **7**. The solid curve is the theoretical susceptibility calculated using eq 2. The dashed curve in (b) is the theoretical susceptibility calculated using eq 2 in ref 33.

contacts of ca. 3.6−3.8 Å, as listed in Table 5. The two dimer units are related by an inversion center. The dimers are stacked along the *c* axis, and are separated by two verdazyl (A and B) cation molecules. The interdimer distance, that is, the distance between Ni(A) and Ni(A′), is 6.693(1) Å for salt **5**. The large AFM exchange interaction ($2J_{A-B}/k_B = -354$ K) observed for salt **5** may be explained by the short interplanar distances of $Ni(dmit)_2$ molecules in the crystal. The $Ni(dmit)_2$ (A) anion molecule connects with the two verdazyl radical cations (V(A) and V(B)) with short intermolecular contacts. Therefore, we can expect some interaction between cation and anion molecules. The difference between the experimental and theoretical values of the susceptibility of salt **5** above 100 K may be due to such an interaction.

In salt **6**, the Ni−Ni distances of the $Ni(dmit)_2$ anions are 4.603(3) Å for the Ni(A)−Ni(B) pair and 6.516(3) Å for the Ni(A)−Ni(C) pair. The short Ni−S, S−S, S−C, and C−C distances were observed for the Ni(A)−Ni(B) pair, as listed in Table 6, indicating dimer formation. Further, short S−S distances were observed for the Ni(A)−Ni(C) pair. In salt **6**, the dimer molecules are sandwiched between two verdazyl cation $[\mathbf{3}]^+$ molecules, forming a linear tetramer ($[\mathbf{3}]^+$−$[Ni(dmit)_2]^-$ (A)−$[Ni(dmit)_2]^-$ (B)−$[\mathbf{3}]^+$) (see Figure 5 and Table 6). There are some comparatively short distances between the V(A) cation and Ni(A) anion, suggesting considerable interaction between the verdazyl radical spin and $Ni(dmit)_2$ anion spin. Therefore, the χ_M of salt **6** was calculated by using eq 2 (that is, the linear tetramer model) in ref 33. The best fit parameters obtained are $2J_1/k_B = -30$ K and $2J_2/k_B = -580$ K, as shown in Figure 10b. The value of the exchange interaction ($2J_1/k_B = -30$ K) between the $Ni(dmit)_2$ anion and verdazyl cation estimated is not so small, but is much smaller than that ($2J_2/k_B = -580$ K) between $Ni(dmit)_2$ anions A and B. Consequently, the susceptibility of salt **6** can be explained by a simple dimer model, as a first-order approximation.

On the other hand, the N*i*−N*j* contacts (*i*, *j* = 1−4) between the nitrogen atoms in the central hydrazidinyl moiety (N1−N2−C7−N3−N4−C8) are larger than 5 Å in salts **5** and **6**, suggesting weak intermolecular exchange interaction ($J_{V^+-V^+}$) between verdazyl cation molecules. In fact, the susceptibilities of salts **5** and **6** below approximately 50 and 100 K can be well described by the Curie−Weiss law with small Weiss constants ($\Theta = -0.4$ and -0.3 K), respectively.

The Lorentzian shape of the single ESR absorption line, which suggests the strong magnetic exchange interaction between the verdazyl cation and $Ni(dmit)_2$ anion spins, was observed for salt **6**. The χ_M of salt **6** was explained by eq 2, as a first-order approximation. In such a case, the temperature dependence of the *g* value of salt **6** is given by eq 4,[34,35]

$$g(T) = [1 - \alpha(T)]g_{V^+} + \alpha(T)g_{Ni^-} \quad (4)$$

where $\alpha(T)$ is the fraction of the susceptibility of the $Ni(dmit)_2$ anion dimer and g_{V^+} and g_{Ni^-} are the *g* values of the verdazyl cation and $Ni(dmit)_2$ anion, respectively.

$$\alpha(T) = \chi_{Ni^-}(T)/[\chi_{V^+}(T) + \chi_{Ni^-}(T)] \quad (5)$$

where $\chi_{V^+}(T)$ and $\chi_{Ni^-}(T)$ correspond to $\chi_{Curie-Weiss}$ and χ_{S-T} in eq 2, respectively. As the *g* values of the cation and anion moieties, we used the *g* values of $[\mathbf{3}]^+I^-$ ($g_{V^+} = 2.0035$ in ethanol) and $[n\text{-}Bu_4N]^+[Ni(dmit)_2]^-$ ($g_{Ni^-} = 2.0472$), respectively. These values are temperature independent. The observed $g(T)$ curve (77 K < *T* < 300 K) can be well reproduced by the effective $g(T)$ value calculated by using eq 4, if we use the relations $\chi_{V^+} = \chi_{Curie-Weiss}$ and $\chi_{Ni^-} = \chi_{S-T}$, as shown in Figure 9c. The result suggests that the spins of cation and anion moieties in salt **6** independently contribute to the magnetic susceptibility.

Similarly, the *g* value of salt **5** decreases from 2.0159 at 300 K to 2.0044 at 77 K by lowering the temperature, as

(34) Tomkiewicz, Y.; Taranko, A. R.; Torrance, J. B. *Phys. Rev. Lett.* **1976**, *36*, 751.
(35) Takahashi, M.; Sugano, T.; Kinoshita, M. *Bull. Chem. Soc. Jpn.* **1984**, *57*, 26.

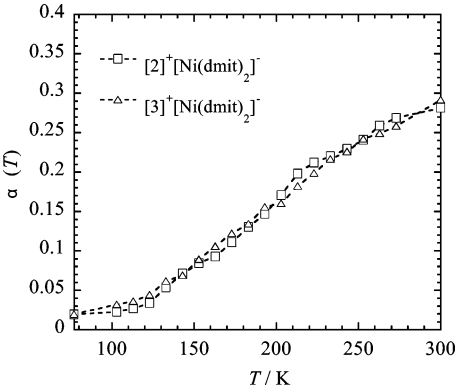

Figure 11. Temperature dependence of the $\alpha(T)$ values for salts **5** and **6**.

shown in Figure 9b. The result shows that both the spins of the verdazyl cation and $Ni(dmit)_2$ anion contribute to the magnetism of salt **5** at 300 K. The *g* value (2.0044) of **5** at 77 K is similar to that (2.0036 in ethanol) of the verdazyl radical cation $[\mathbf{2}]^+$, indicating that the spins of the verdazyl cation contribute mainly to the χ_M of salt **5** at 77 K. As shown in Figure 9b, the temperature dependence of the *g* value cannot be explained by eq 4, if we use the value of $2J/k_B = -354$ K obtained by the susceptibility measurement. There are two reasons for the inaccordance: (i) we cannot determine the correct *g* values for salt **5** because the Curie impurity signal of the radical cation overlaps the signal of salt **5**, and (ii) the value of the exchange interaction determined by the susceptibility measurement is not correct, because of the interaction between the $Ni(dmit)_2$ and verdazyl cation molecules. However, the detailed reason is not clear at present.

As shown in Figure 11, the values of $\alpha(T)$ for salts **5** and **6** are 0.281 and 0.292 at 300 K, respectively. The values decrease by lowering the temperature and approach zero at 77 K, suggesting that the contributions of $Ni(dmit)_2$ anion spins to the susceptibility disappear almost at 77 K in these salts. The AFM exchange interactions between $Ni(dmit)_2$ anion molecules are strong for these salts.

Magnetic Property of Salt 7. As described in a previous section, the value of $\chi_M T$ for the 1:3 salt **7** is 0.642 (K emu)/mol at 300 K, and decreases by lowering the temperature, as shown in Figure 7. The magnetic behavior is similar to that of salts **5** and **6**. As shown in Figure 10, the experimental curve can be approximately reproduced by the two-term contributions (eq 2) with (i) $C = 0.376$ (K emu)/mol and $\Theta = -1.7$ K and (ii) $2J/k_B = -258$ K. The difference between the experimental and theoretical values of susceptibility may be due to the interaction between the verdazyl cation and $[Ni(dmit)_2]_3^-$ anion spins. We can expect stronger AFM exchange interaction between the $[Ni(dmit)_2]_3^-$ anion molecules than that between verdazyl radical cations, as observed for salts **4**−**6**. Therefore, the susceptibility of salt **7** below ca. 30 K is due to the spins of the verdazyl radical cation.

Several kinds of 1:3 complexes (cation)$[Ni(dmit)_2]_3$ of a closed-shell cation with $Ni(dmit)_2$ species have been prepared, and the structural and conducting properties have been studied.[9,36,37] The complexes show semiconducting and metallic behavior. The $Ni(dmit)_2$ units generally form trimers. However, the magnetic properties of the complexes have not been reported, as far as we know. On the other hand, in the case of the crystal of $(TPP)[Ni(dmit)_2]_3$ (TPP = tetraphenylphosphonium), two of the three $Ni(dmit)_2$ units form columns, the remaining unit exists almost perpendicular to the stack, and the conducting sheets of the $Ni(dmit)_2$ anions are separated by layers of large countercations.[38] The susceptibility follows Curie−Weiss law with $C = 0.40$ (K emu)/mol and $\Theta = 1.6$ K. The Curie constant corresponds to one spin per three $Ni(dmit)_2$ units. The result obtained for salt **7** also suggests the existence of one spin per three $Ni(dmit)_2$ units. However, the exchange interaction ($2J/k_B = -258$ K) observed is much larger than that in the $(TPP)[Ni(dmit)_2]_3$ complex. Crystal structure analysis of salt **7** is necessary to discuss the difference in the magnetic properties.

Conducting Properties of Salts 4−7. As described in a previous section, the three 1:1 salts **4**−**6** are insulators, as expected for the 1:1 complexes. On the other hand, the 1:3 salt **7** is a semiconductor ($\sigma_{RT} = 0.10$ S cm^{-1}) with activation energy $E_A = 0.10$ eV. The result indicates that salt **7** is a new molecular paramagnetic semiconductor.

Recently, we reported the first example of 1:1 and 1:3 salts of the $Ni(dmit)_2$ anion with the 6-oxoverdazyl radical cation $[V]^+$ (V = 3-[4-(diethylmethylammonio)phenyl]-1,5-diphenyl-6-oxoverdazyl radical).[28] The χ_M of the 1:1 salt $[V]^+[Ni(dmit)_2]^-$ was explained by the sum of the contributions from (i) a Curie−Weiss system ($\Theta = -1.6$ K) and (ii) the one-dimensional Heisenberg AFM alternating-chain system with $2J_{A-B}/k_B = -274$ K (alternation parameter $\alpha = J_{A-C}/J_{A-B} = 0.2$). The χ_M of the 1:3 salt was also explained by the two-term contributions from (i) the Curie−Weiss system ($\Theta = -5.0$ K) and (ii) the dimer system with $2J/k_B = -258$ K. The 1:1 and 1:3 salts were a paramagnetic insulator and semiconductor, respectively. The structural, magnetic, and conducting properties of the salts reported are similar to those obtained in the present work. The magnetic interactions between the verdazyl radical cations and between the verdazyl cation and $Ni(dmit)_2$ anion observed were weaker than expected, except for the case of salt **4**. To obtain the organic/inorganic hybrid system which shows the ferromagnetism (or antiferromagnetism) and superconductivity (or metallic conductivity), it is necessary to use the different types of verdazyl radical cations with smaller molecular size, such as 1,5-dimethyl-6-oxo- and 1,5-dimethyl-6-thioxoverdazyls, for which we can expect stronger magnetic interaction.[13,19,20]

Summary

In the present work, four magnetic charge-transfer salts (**4**−**7**) of 3-[4-(trimethylammonio)phenyl]-1,5-diphenyl-6-oxoverdazyl radical cation ($[\mathbf{1}]^+$) and its mono- and dimethyl derivatives ($[\mathbf{2}]^+$ and $[\mathbf{3}]^+$) with $[Ni(dmit)]^-$ and $[Ni(dmit)_2]_3^-$

(36) Verdhuizen, Y. S. J.; Smeets, W. J. J.; Veldman, N.; Spek, A. L.; Faulmann, C.; Auban-Senzier, P.; Jerome, D.; Paulus, P. M.; Haasnoot, J. G.; Reedijk, J. *Inorg. Chem.* **1997**, *36*, 4930.
(37) Xu, W.; Zhang, D.; Yang, C.; Jin, X.; Li, Y.; Zhu, D. *Synth. Met.* **2001**, *122*, 409.
(38) Nakamura, T.; Underhill, A. E.; Coomber, A. T.; Friend, R. H.; Tajima, H.; Kobayashi, A.; Kobayashi, H. *Inorg. Chem.* **1995**, *34*, 870.

anions ([**1**]$^+$[Ni(dmit)$_2$]$^-$ (**4**), [**2**]$^+$[Ni(dmit)$_2$]$^-$ (**5**), [**3**]$^+$[Ni(dmit)$_2$]$^-$ (**6**), and [**1**]$^+$[Ni(dmit)$_2$]$_3^-$ (**7**)) have been prepared, and their structural, magnetic, and conducting properties have been studied. The results of the crystal structure analyses of the 1:1 salts **4**−**6** indicate dimer formation of the Ni(dmit)$_2$ anion moiety in the salts. The separate contributions of the verdazyl cation ($S = 1/2$) and Ni(dmit)$_2$ anion ($S = 1/2$) subsystems to the total magnetic susceptibility of the salts were evaluated from the measurements of the temperature dependence of the susceptibility ($\chi_M(T)$) and the g value ($g(T)$) of the 1:1 salt **5** and the 1:3 salt **7**. Fraction $\alpha(T)$ values of the Ni(dmit)$_2$ anion in the susceptibility of salts **5** and **6** decrease by lowering the temperature, and approach zero at 77 K, suggesting that the magnetic gaps of the spin pair in the Ni(dmit)$_2$ anion in the salts are larger than those in the verdazyl cation. On the other hand, the magnetic susceptibilities of salts **4** and **6** were explained by the four-spin linear tetramer model ([**1** (or **3**)]$^+$−Ni(dmit)$_2$−Ni(dmit)$_2$−[**1** (or **3**)]$^+$). The 1:1 salts **4**−**6** are insulators. On the other hand, the 1:3 salt **7** is a semiconductor. The examples of the organic/inorganic hybrid system which shows magnetism and conductivity are very limited, because of the difficulty in the molecular design of the complexes. The present work provides an example of a new molecular paramagnetic semiconductor consisting of an open-shell verdazyl radical cation and a metal complex anion.

Acknowledgment. We are very grateful to Prof. K. Tanaka and Mr. T. Nakayashiki of Kyoto University for their kind help in the measurement of conductivity. We are also very grateful to Dr. K. Suzuki of the Institute for Molecular Science and Prof. T. Ishida of the University of Electro-Communications for their kind help in the SQUID measurements and the analysis of the susceptibility of salt **4**, respectively. We are also very grateful to Prof. T. Sugano of Meiji Gakuin University for his helpful discussions. This work was partly supported by a Grant-in-Aid for Scientific Research on Priority Areas (B) of Molecular Conductors and Magnets (Area No. 730/11224205) from the Ministry of Education, Science, Sports and Culture, Japan. This work was supported by the Joint Studies Program (2000−2002) of the Institute for Molecular Science.

Supporting Information Available: Tables listing detailed crystallographic data, atomic positional parameters, and bond lengths and angles of salts **4**−**6** and **8** in CIF format. This material is available free of charge via the Internet at http://pubs.acs.org.

IC030068Q